



## Advanced Composite Materials

Publication details, including instructions for authors and subscription information:

<http://www.tandfonline.com/loi/tacm20>

### Enhancement of PVDF's piezoelectricity by VGCF and MWNT

Liangke Wu<sup>a,b</sup>, Weifeng Yuan<sup>c</sup>, Takaya Nakamura<sup>a</sup>, Satoshi Atobe<sup>d</sup>, Ning Hu<sup>a,c</sup>, Hisao Fukunaga<sup>d</sup>, Christiana Chang<sup>e</sup>, Yutaka Zemba<sup>f</sup>, Yuan Li<sup>g</sup>, Tomonori Watanabe<sup>a</sup>, Yaolu Liu<sup>a</sup>, Alamusi<sup>a</sup>, Huiming Ning<sup>a</sup>, Jinhua Li<sup>a</sup>, Hao Cui<sup>a</sup> & Yajun Zhang<sup>h</sup>

<sup>a</sup> Department of Mechanical Engineering, Chiba University, 1-33 Yayoi-cho, Inage-ku, Chiba, 263-8522, Japan

<sup>b</sup> Department of Mechanical Engineering, Zhejiang University, 38 Zheda Road, Hangzhou, 310027, P.R. China

<sup>c</sup> School of Manufacturing Science and Engineering, Southwest University of Science and Technology, 59 Qinglong Road, Mianyang, 621010, P.R. China

<sup>d</sup> Department of Aerospace Engineering, Tohoku University, 6-6-01 Aramaki-Aza-Aoba, Aoba-ku, Sendai, 980-8579, Japan

<sup>e</sup> Department of Mechanical Engineering, University of Houston, 4800 Calhoun Road, Houston, TX, 77004, USA

<sup>f</sup> Sougou Sekkei Co., Ltd., 21-F, Sekaiboeki Center Bldg., 2-4-1 Hamamatsu-cho, Minato-ku, Tokyo, 105-6121, Japan

<sup>g</sup> Department of Nanomechanics, Tohoku University, 6-6-01 Aramaki-Aza-Aoba, Aoba-ku, Sendai, 980-8579, Japan

<sup>h</sup> College of Mechanical and Electrical Engineering, Beijing University of Chemical Technology, Beishanhuang Dong Lu 15, Chaoyang District, Beijing, 100029, China

Published online: 05 Feb 2013.

To cite this article: Liangke Wu, Weifeng Yuan, Takaya Nakamura, Satoshi Atobe, Ning Hu, Hisao Fukunaga, Christiana Chang, Yutaka Zemba, Yuan Li, Tomonori Watanabe, Yaolu Liu, Alamusi, Huiming Ning, Jinhua Li, Hao Cui & Yajun Zhang (2013) Enhancement of PVDF's piezoelectricity by VGCF and MWNT, *Advanced Composite Materials*, 22:1, 49-63, DOI: [10.1080/09243046.2013.764780](http://dx.doi.org/10.1080/09243046.2013.764780)

To link to this article: <http://dx.doi.org/10.1080/09243046.2013.764780>

Taylor & Francis makes every effort to ensure the accuracy of all the information (the "Content") contained in the publications on our platform. However, Taylor & Francis, our agents, and our licensors make no representations or warranties whatsoever as to the accuracy, completeness, or suitability for any purpose of the Content. Any opinions and views expressed in this publication are the opinions and views of the authors, and are not the views of or endorsed by Taylor & Francis. The accuracy of the Content should not be relied upon and should be independently verified with primary sources of information. Taylor and Francis shall not be liable for any losses, actions, claims, proceedings, demands, costs, expenses, damages, and other liabilities whatsoever or howsoever caused arising directly or indirectly in connection with, in relation to or arising out of the use of the Content.

This article may be used for research, teaching, and private study purposes. Any substantial or systematic reproduction, redistribution, reselling, loan, sub-licensing, systematic supply, or distribution in any form to anyone is expressly forbidden. Terms & Conditions of access and use can be found at <http://www.tandfonline.com/page/terms-and-conditions>

## Enhancement of PVDF's piezoelectricity by VGCF and MWNT

Liangke Wu<sup>a,b</sup>, Weifeng Yuan<sup>c</sup>, Takaya Nakamura<sup>a</sup>, Satoshi Atobe<sup>d</sup>, Ning Hu<sup>a,c\*</sup>, Hisao Fukunaga<sup>d</sup>, Christiana Chang<sup>e</sup>, Yutaka Zemba<sup>f</sup>, Yuan Li<sup>g</sup>, Tomonori Watanabe<sup>a</sup>, Yaolu Liu<sup>a</sup>, Alamusi<sup>a</sup>, Huiming Ning<sup>a</sup>, Jinhua Li<sup>a</sup>, Hao Cui<sup>a</sup> and Yajun Zhang<sup>h</sup>

<sup>a</sup>Department of Mechanical Engineering, Chiba University, 1-33 Yayoi-cho, Inage-ku, Chiba 263-8522, Japan; <sup>b</sup>Department of Mechanical Engineering, Zhejiang University, 38 Zheda Road, Hangzhou 310027, P.R. China; <sup>c</sup>School of Manufacturing Science and Engineering, Southwest University of Science and Technology, 59 Qinglong Road, Mianyang 621010, P.R. China; <sup>d</sup>Department of Aerospace Engineering, Tohoku University, 6-6-01 Aramaki-Aza-Aoba, Aoba-ku, Sendai 980-8579, Japan; <sup>e</sup>Department of Mechanical Engineering, University of Houston, 4800 Calhoun Road, Houston, TX 77004, USA; <sup>f</sup>Sougou Sekkei Co., Ltd., 21-F, Sekaiboeki Center Bldg., 2-4-1 Hamamatsu-cho, Minato-ku, Tokyo 105-6121, Japan; <sup>g</sup>Department of Nanomechanics, Tohoku University, 6-6-01 Aramaki-Aza-Aoba, Aoba-ku, Sendai 980-8579, Japan; <sup>h</sup>College of Mechanical and Electrical Engineering, Beijing University of Chemical Technology, Beishanhuang Dong Lu 15, Chaoyang District Beijing 100029, China

(Received 20 July 2012; accepted 7 January 2013)

Multi-walled carbon nanotube (MWNT) and vapor grown carbon fiber (VGCF) were blended into poly (vinylidene fluoride) (PVDF) to enhance the piezoelectricity of the neat polymer. The PVDF composite films were prepared by solution casting method, stretched uniaxially and poled in silicon oil. The nanofiller contents range from 0.05 to 0.3 wt.%. Open circuit output voltage and energy harvesting tests indicate that both the PVDF/MWNT and PVDF/VGCF composite films approached the maximum output at the nanofiller content of 0.05 wt.%. Compared to the neat PVDF films, the maximum increasing rates of open circuit voltage and harvested power density are 24% and 47% for the PVDF/MWNT films and 15% and 78% for the PVDF/VGCF films, respectively. X-ray diffraction analysis showed an increase in content of the  $\beta$  phase in the PVDF composites; thus, the piezoelectric properties, which are dependent on  $\beta$  phase content, were enhanced. Stretching of the films leads to the transformation of PVDF from  $\alpha$  phase to  $\beta$  phase form. Moreover, the addition of nanofillers, such as MWNT and VGCF, improves this transformation since the nanofillers provide a phase transformation nucleation function.

**Keywords:** piezoelectricity; MWNT; VGCF; PVDF; composite; energy harvesting

### 1. Introduction

Energy harvesting devices are appealing for systems in which the replacement of batteries is inconvenient and costly. Excellent inherent piezoelectric and pyroelectric properties make poly (vinylidene fluoride) (PVDF) a potential membrane material for energy harvesting devices.[1] The PVDF is a semicrystalline polymer and its polymer chain exists in at least four forms, i.e.  $\alpha$  (form II),  $\beta$  (form I),  $\gamma$  (form III), and  $\delta$  (form IV).[2–3]

---

\*Corresponding author. Email: [huning@faculty.chiba-u.jp](mailto:huning@faculty.chiba-u.jp)

The  $\alpha$  crystal, which possesses a monoclinic unit cell with trans-gauche-trans- gauche' (TGTG') chain conformation, is the most common polymorph. Usually, the  $\alpha$  phase is directly obtained from the initial crystallization of melt. However, the  $\beta$  phase, which possesses an orthorhombic unit cell with all trans (TTTT) conformation, is the most important polymorph because it possesses piezoelectric and pyroelectric properties due to its dipolar conformation. [3–5]

As the piezoelectricity of PVDF depends on the  $\beta$  phase content, several methods have been developed to promote the formation of the  $\beta$  phase during fabrication. According to previous work,  $\beta$  phase can be obtained by drawing,[6,7] poling at high voltage,[8,9] crystallization under high pressure,[10,11] polymer blending,[12] etc. Moreover, addition of various nanofillers is a widely used method to improve PVDF's properties. Since the nanofillers can affect the crystallization process extensively, a slight addition of nanofiller can significantly influence the magnetic,[13] electrical,[13–15] mechanical,[16,17] thermal,[17] piezoelectric, [18–21] and ferroelectric [21] properties of PVDF. Especially, the phase transformation caused by the addition of carbon nanofiber (CNF) [14] and multi-walled carbon nanotube (MWNT) [17,22,23] in PVDF has been investigated. Although some progresses have been made, the mechanism of phase transformation, the interaction between PVDF and various nanofillers, and the control of the crystallization process have not been studied in detail. Also, a few investigations on piezoelectricity were only limited to PVDF/MWNT composites, e.g. [20,21]. To date, there has been no report on the properties of voltage output and energy harvesting of PVDF/MWNT and PVDF/CNF composites.

In this study, in order to increase the piezoelectricity of PVDF, MWNT and vapor grown carbon fiber (VGCF) were used as nanofillers in the PVDF matrix, respectively. As mentioned above, the nanofillers can improve the formation of  $\beta$  phase, which leads to higher piezoelectricity. Different nanofillers with different sizes and physical properties may affect the crystallization and phase transformation processes, leading to different piezoelectric properties. We focus on the different improvement effects of the MWNT and VGCF on the PVDF phase transformation, the open circuit voltage and the energy harvesting capability.

## 2. Experiments and results

### 2.1. Preparation of PVDF/MWNT and PVDF/VGCF composites

#### 2.1.1. Materials

The matrix is poly ((vinylidene fluoride)-co-hexafluoropropylene) (PVDF-HFP), (Arkema Inc. Kynar Flex 2801). The solvent is *N, N*-dimethylformamide (DMF) (Wako Pure Chemical Industries, Ltd.). The nanofillers are MWNT (Nano carbon technology Ltd. MWNT-7) and VGCF (Showa Denko Ltd. VGCF<sup>TM</sup>). Some properties of the two nanofillers are shown in Table 1. Due to their comparatively large sizes within various nanomaterials, they can be easily distributed uniformly in the matrix material at low contents. Note that the diameter of the VGCF is much larger than that of the MWNT, but its purity is comparatively lower.

Table 1. Properties of MWNT and VGCF.

Properties	MWNT	VGCF
Fiber diameter (nm)	40–90	150
Fiber length ( $\mu\text{m}$ )	10–30	8–15
Purity (%)	>99.5	>99

### 2.1.2. Preparation process

The solution-cast method was used to prepare PVDF films, as it is easy and is of low cost. The process mainly includes three steps, i.e. film creation, uniaxially stretching, and poling. As illustrated in Figure 1, it can be described as follows:

- (1) The MWNT or VGCF was dispersed into the melting agent, DMF, by using an ultra-sound dispersion machine for 15 min.
- (2) The PVDF powder was poured into the mixture solution and then the solution was stirred by a planetary centrifugal mixer at 2000 rpm for 10 min. The mass ratio of (PVDF + Nanofiller): DMF was 1:3.
- (3) The nanofiller/PVDF/DMF mixture solution was sonicated for 5 min and mechanically stirred by the planetary centrifugal mixer at 2000 rpm for 10 min and then defoamed for 1 min.
- (4) The final mixture was poured onto an aluminum (Al) plate and was made into thick films in a detachable mold. Then, the Al plate was heated to 90 °C for removing the DMF. After drying, uniformly thick composite films were obtained.
- (5) The films were stretched by a universal testing machine. The drawing rate was 10 mm/min, and the final elongation was 400–500% at around 60 °C.
- (6) After drawing, the poling process was carried out in silicone oil at room temperature by a step-wise poling.[24] This method increases the applied voltage on the composite films by small step increments. The poling electric field ranged from 20 to 60 MV/m, increasing in 10 MV/m increments. The poling interval was 8 min, the pause time was 4 min, and the number of steps was set to 5.

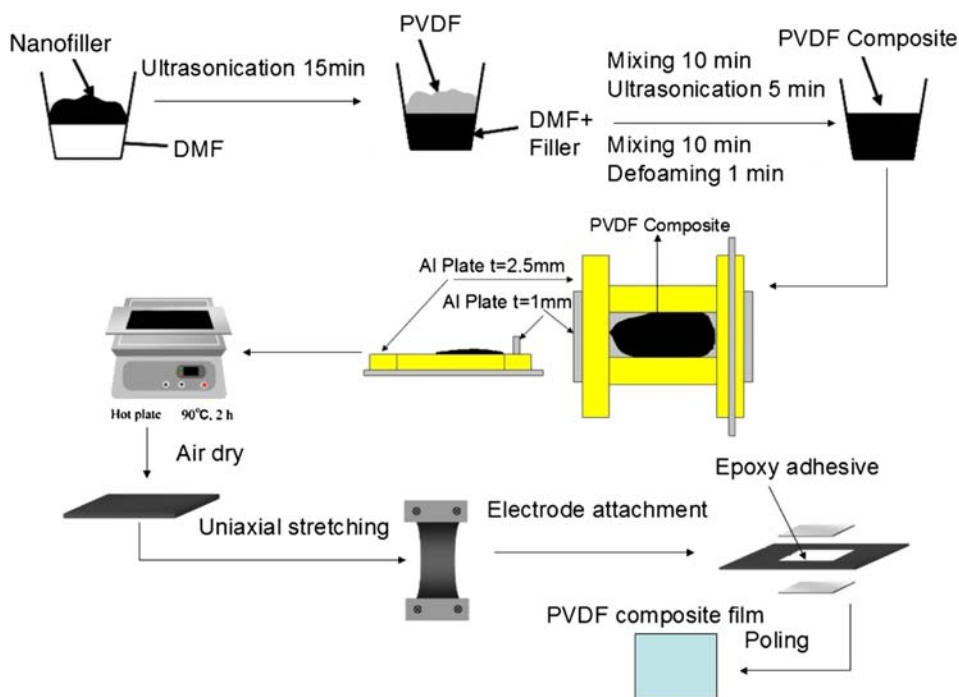


Figure 1. Preparation procedure of PVDF composite films.

The nanofiller contents of films were 0, 0.05, 0.2, and 0.3 wt.%. For simplicity, the samples will be referred to as PVDF, PVDF/MWNT(0.05), PVDF/MWNT(0.2), PVDF/MWNT(0.3), PVDF/VGCF(0.05), PVDF/VGCF(0.2), and PVDF/VGCF(0.3). The average thickness of the films with different contents was around 90  $\mu\text{m}$ .

## 2.2. Open circuit measurement

### 2.2.1. Experiments

As illustrated in Figure 2, the prepared PVDF composite films were attached onto an Al beam to test the open circuit output voltage under dynamic strain. A 25 Hz sinusoidal current created by a function generator was applied to an electromagnet and the induced magnetic field attracted or repelled a magnet (not shown) attached on the Al beam, resulting in oscillation of the Al beam. Due to strain from the bending beam, voltage was produced between the two electrodes due to the piezoelectricity of the PVDF composite films. To evaluate the properties of the films effectively, the tip displacement of the beam measured by a laser displacement sensor was approximately maintained at 1 mm. The open circuit output voltage was recorded by an oscilloscope and sent to a computer.

### 2.2.2. Results

The stress/charge relationship of a piezoelectric element ('31' mode, where '3' is the film thickness direction and '1' is the length direction of the beam or film) is shown in Figure 3.

The relationship between stress  $T_1$ , strain  $S_1$ , electric field  $E_3$ , and electric flux density  $D_3$  is given by

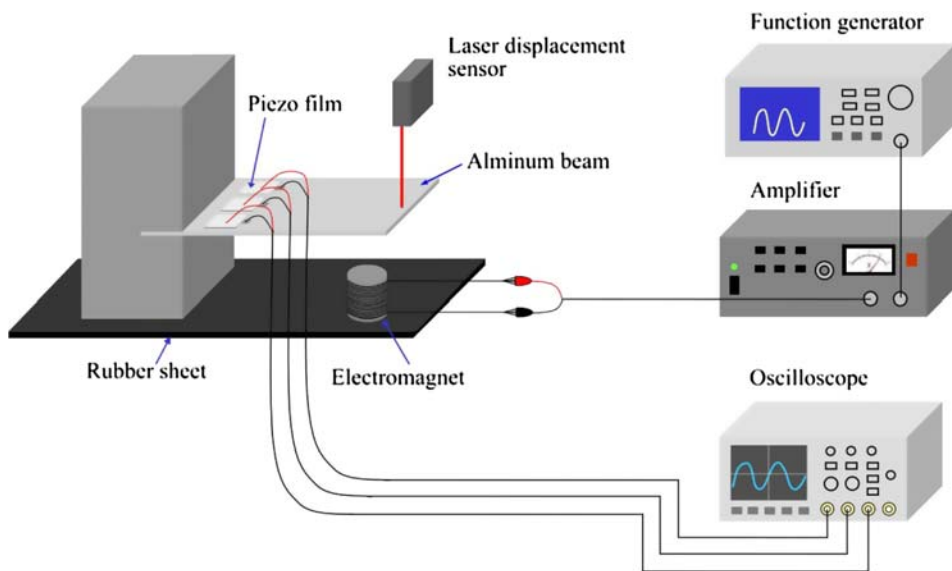


Figure 2. Experimental setup of open circuit measurement.

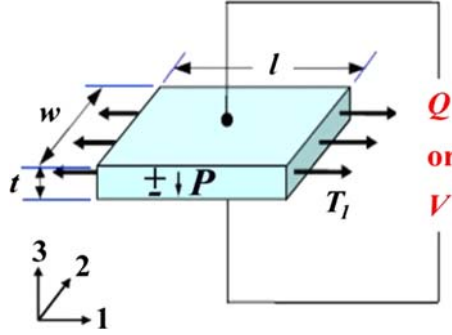


Figure 3. Stress/charge relationship of piezoelectric element.

$$\begin{cases} S_1 = S_{11}^E T_1 + d_{31} E_3 \\ D_3 = d_{31} T_1 + \varepsilon_{33}^T E_3. \end{cases} \quad (1)$$

in which  $S_{11}^E$  is the compliance of the short circuit piezoelectric element,  $d_{31}$  is the piezoelectric strain constant, and  $\varepsilon_{33}^T$  is the permittivity when the stress is 0. In the experiments,  $E_3$ , the electric field along the three directions is 0, so we can obtain the following equation

$$D_3 = d_{31} T_1 = \frac{Q}{A_{\text{ele}}}. \quad (2)$$

in which  $A_{\text{ele}}$  is the area of the electrode. Then, the charge between the two surfaces of the film can be expressed by

$$Q = A_{\text{ele}} T_1 d_{31}. \quad (3)$$

We express the capacitance of the film as  $C_0$ , Young's modulus as  $E'$ , the corresponding strain in the 1 direction as  $\varepsilon'$ , the piezoelectric voltage constant as  $g_{31}$ , and the displacement along the 1 direction as  $\Delta l$ . Then, the open circuit voltage between the two surfaces of the film is given as

$$V = \frac{Q}{C_0} = \frac{T_1 d_{31} t}{\varepsilon_{33}^T} = E' \varepsilon' g_{31} t = \frac{E' g_{31} \Delta l t}{l} \quad (4)$$

According to Equation (4), the output voltage  $V$  is proportional to the strain  $\varepsilon'$  at the measurement location, or the deflection of the free beam tip.

The effective or root-mean-square voltage  $V_{\text{rms}}$  of a generated output voltage  $V$  within a time period  $t_{\text{max}}$  is defined as

$$V_{\text{rms}} = \sqrt{\int_0^{t_{\text{max}}} \frac{V^2 dt}{t_{\text{max}}}} \quad (5)$$

For a sinusoidal  $V$ , there is:  $V_{\text{rms}} = 0.707 V_{\text{max}}$ , where  $V_{\text{max}}$  is the amplitude of  $V$ .

Three films with the same nanofiller content were attached on the same beam (Figure 2) and their open circuit voltages were independently measured. Since the thickness,  $t$ , and the free-end displacement,  $u$ , are slightly different between films and between beams, for direct

comparison, we define  $t_0 = 100 \mu\text{m}$  and  $u_0 = 1 \text{ mm}$  as the standard film thickness and standard beam free-end displacement, respectively. Then, the effective voltage can be transformed to a calibrated voltage,  $V_c$ , following the equation

$$V_c = \frac{V_{\text{rms}}}{\left(\frac{u}{t_0 u_0}\right)} \quad (6)$$

The open circuit output voltages for various samples of the same content were calculated and averaged. The final results are shown in Figure 4. It can be seen that a suitable addition of MWNT or VGCF enhances the open circuit output voltages or piezoelectric properties of PVDF. In Figure 4, when the VGCF content is 0.05 wt.%, there is a peak open circuit voltage of PVDF/VGCF film, which is 15% higher than that of pure PVDF films. However, at the content of 0.3 wt.%, the open circuit voltage decreases about 30% from the peak value. Thus, the optimal nanofiller content may be between 0.05 and 0.2 wt.%. Similarly, the PVDF/MWNT film at 0.05 wt.% loading has the maximum increase of open circuit voltage, i.e. 24%, compared to the pure PVDF films. Compared to the PVDF/VGCF film, the higher maximum open circuit voltage of the PVDF/MWNT film may be caused by the present MWNT's higher purity (Table 1) and electrical conductivity by inference from the following evidences. In the authors' recent work,[25] it was identified that the electrical conductivity of the present MWNT-based epoxy composites is much higher than that of VGCF/epoxy composites at the same addition level. Moreover, we found [26] that reduced graphene oxide with a high electrical conductivity is much more effective than insulated graphene oxide for improving the piezoelectric properties of PVDF.

As reported in [21], the maximum increment of  $d_{31}$  is 10% at 0.2 wt.% addition of MWNT. From Equations (3) and (4), the increase of open circuit voltage can be caused by the increased  $d_{31}$  if there is no decrease in the capacitance  $C_0$  (or permittivity  $\epsilon_{33}^T$ ), and no increase in the stress  $T_1$ . Therefore, the  $d_{31}$  of the present PVDF/VGCF (0.05) and PVDF/MWNT (0.05) films should be higher than that in [21]. The MWNT used in [21] has the purity of 95% and the diameter of 10–15 nm. Its lower purity (or lower electrical conductivity) and poor dispersion caused by its very small sizes may result in the increase of the optimal nanofiller content, i.e. 0.2 wt.% [21] compared to the present one, i.e. 0.05 wt.% for both

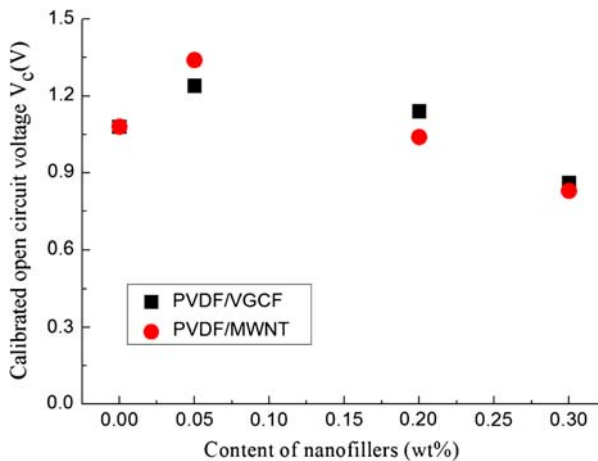


Figure 4. Calibrated open circuit output voltages of PVDF/MWNT and PVDF/VGCF films.

PVDF/VGCF and PVDF/MWNT films. Moreover, from Equation (4), if the increase of  $E'$  for the composite films can be neglected due to extremely low nanofiller additions, the increase of open circuit voltage implies the increase of piezoelectric voltage constant  $g_{31}$  due to addition of nanofillers.

### 2.3. Energy harvesting measurements

#### 2.3.1. Experiments

The setup for the energy harvesting measurements is similar to that for open circuit output voltage measurements, but the open circuit is replaced by an AC circuit, as shown in Figure 5.

Similar to the open circuit experiments, three identical content samples were attached to the Al plate and excited at the primary resonant frequency. In the energy harvesting experiments, we strictly controlled the free-tip displacement to be 2.5 mm for all beams. Under the above conditions, the total harvested power generated by the three films with the same nanofiller loading was measured. Then, the power produced per unit volume, i.e. power density, was calculated and used for comparison between various nanofiller loadings.

#### 2.3.2. Results

The total power of the circuit and the average harvested power density are calculated by

$$P = \frac{V_{\text{rms}}^2}{R}, D_{\text{avr}} = \frac{P}{V_{\text{ol}}} \quad (7)$$

in which  $P$  is the total harvested power of the three piezoelectric films,  $V_{\text{rms}}$  is the root-mean-square of voltage (see Equation (5)),  $R$  is the resistance load,  $D_{\text{avr}}$  is the average harvested power density, and  $V_{\text{ol}}$  is the total volume of the three piezoelectric films.

The results for the different nanofiller loadings are shown in Figures 6 and 7. From these figures, it can be seen that the average harvested power density of PVDF/MWNT(0.05) films is 47% higher than that of pure PVDF films. Furthermore, the average harvested power density of PVDF/VGCF (0.05) is 78% higher than that of pure PVDF films, which is also much higher than that of PVDF/MWNT films.

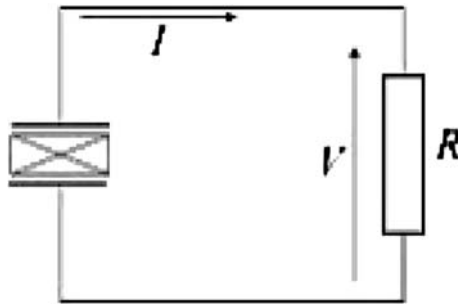


Figure 5. Standard AC circuit.

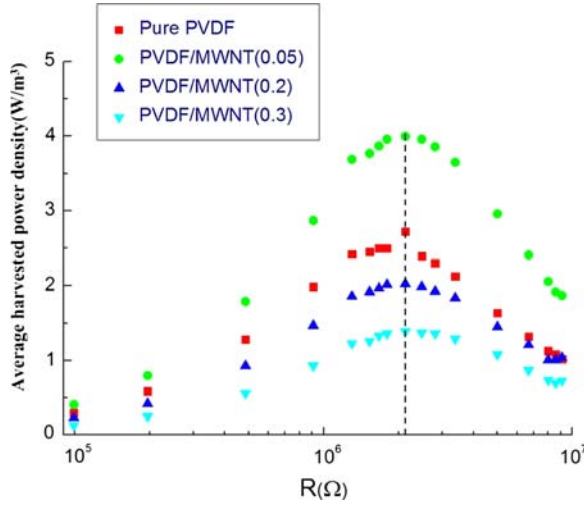


Figure 6. Average harvested power density for beam with three bonded PVDF/MWNT composite patches excited at resonance with standard AC (beam free-end displacement is 2.5 mm).

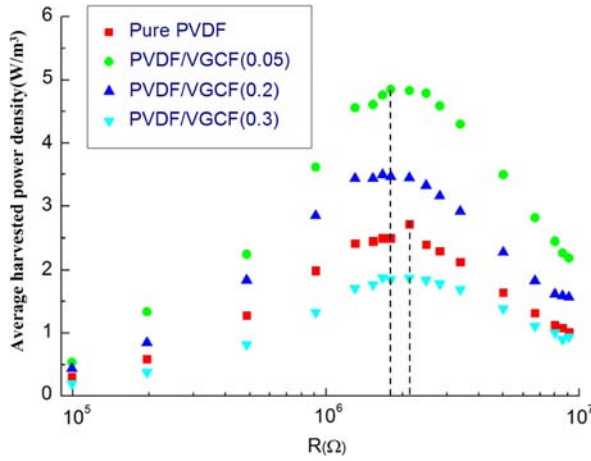


Figure 7. Average harvested power density for beam with three bonded PVDF/VGCF composite patches excited at resonance with standard AC (beam free-end displacement is 2.5 mm).

### 2.3.3. Discussion

A theoretical representation of the energy harvesting scheme is given by the model proposed by Guyomar et al. [27]. The piezoelectric energy harvesting structure is illustrated in Figure 8.

For a standard AC device, the power can be expressed by

$$P = \frac{R\alpha^2}{1 + (RC_0\omega)^2} \frac{F_m^2}{2C^2} \quad (8)$$

and the optimal resistance and maximum power are

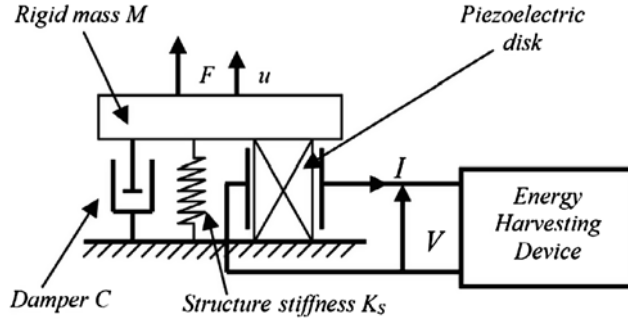


Figure 8. Schematic of energy harvesting device.

$$R_{\text{opt}} = \frac{1}{C_0 \omega}, P_{\text{max}} = \frac{\alpha^2}{4C_0 \omega} \frac{F_m^2}{C^2} \quad (9)$$

where,  $R$  is the load resistance,  $C_0$  the clamped capacitance of the piezoelectric element,  $\omega$  the angular frequency,  $F_m$  the external force amplitude,  $C$  the damper corresponding to the mechanical losses of the structure, and  $\alpha$  the force factor,  $e_{31}$  the piezoelectric constant,  $C_0$ , and  $\alpha$  can be expressed by

$$\alpha = e_{31} w, C_0 = \epsilon_{33}^S \frac{wl}{t} \quad (10)$$

Then, Equation (8) can be rewritten as

$$P = R \frac{e_{31}^2 w^2}{1 + (RC_0 \omega)^2} \frac{F_m^2}{2C^2} \quad (11)$$

where,  $w$ ,  $l$  and  $t$  are the width, length and thickness of the piezoelectric element, respectively, and  $\epsilon_{33}^S$  is the clamped permittivity of the piezoelectric element. If the piezoelectric element is vibrated near the primary resonance frequency, the relationship of  $\alpha$  and  $C_0$  can be expressed as

$$\alpha = \gamma C_0 \quad (12)$$

where,  $\gamma$  is the ratio of the piezoelectric open circuit voltage to the beam free-end displacement.

*Discussion of PVDF/MWNT composite films.* From Figure 6 (dash line), we know that the optimal resistance  $R_{\text{opt}}$  of the PVDF/MWNT composite films remains the same compared with that of neat PVDF films. In experiment, the angular frequency  $\omega$  is nearly the same, according to Equation (9), and  $C_0$  also remains unchanged for the films with different MWNT contents. For PVDF/MWNT samples, their average thickness  $t$ , width  $w$ , and length  $l$  are almost the same with those of pure PVDF films; then, from Equation (10), it can be estimated that there is no obvious change in the clamped permittivity  $\epsilon_{33}^S$ . Since the damper,  $C$ , and the external force amplitude,  $F_m$ , generally remain unchanged in the experiments, the increment of power mainly results from an increase in the force factor,  $\alpha$  (see Equation (9)).

Furthermore, according to Equations (10) and (11), the increase in the output power is mainly due to an increase of  $e_{31}$ .

The piezoelectric output voltage constant is defined as

$$g_{31} = \frac{d_{31}}{\varepsilon_{33}^T} \quad (13)$$

According to Equation (11),  $P$  is proportional to  $e_{31}^2$ ; also, according to Equation (7),  $P$  is proportional to  $V_{\text{rms}}^2$ . Thus,  $e_{31}$  is proportional to  $V_{\text{rms}}$ . From Equation (4), we can know that  $V_{\text{rms}}$  is also proportional to  $g_{31}$ . Therefore,  $g_{31}$  increases, which is proportional to  $e_{31}$ . Moreover, since there is the relationship between the piezoelectric constant vector  $\mathbf{e}$  and the piezoelectric strain constant vector  $\mathbf{d}$  as:  $\mathbf{e} = \mathbf{C}^E \mathbf{d}$  with the elastic stiffness tensor  $\mathbf{C}^E$ . By neglecting the variation of  $\mathbf{C}^E$ , the increase of  $e_{31}$  leads to the increase of  $d_{31}$ .

*Discussion of PVDF/VGCF composite films.* As shown previously, although the open circuit output voltage of the PVDF/VGCF (0.05) films is lower than that of the PVDF/MWNT (0.05) films, its average harvested power density is higher. This phenomenon can be explained in the following. From Figure 7, it can be concluded that the optimal resistance  $R_{\text{opt}}$  of PVDF/VGCF (0.05) films is less than that of pure PVDF films. From Equations (9) and (10), since the angular frequency remains the same, the decrease of the optimal resistance  $R_{\text{opt}}$  in the PVDF/VGCF (0.05) films should be caused by the increase of the clamped capacitance  $C_0$  or the permittivity  $\varepsilon_{33}^S$  if  $w$ ,  $l$ , and  $t$  are constant. In fact, it was reported that the addition of MWNT will increase the permittivity of PVDF.[15,23]

According to Equations (9), (10), and (12),  $\alpha$  and  $e_{31}$  also increased. As discussed above, for the case of PVDF/MWNT films, the addition of VGCF will also improve  $g_{31}$ .

Therefore, we come to the conclusion

$$C'_0 = mC_0, \quad g'_{31} = ng_{31} \quad (m, n > 1) \quad (14)$$

where, the properties of the PVDF/VGCF(0.05) films are marked by “'”.

Combining Equations (4), (10), (12), and (14), the parameters of PVDF/VGCF films will be

$$V' = nV, \quad \gamma' = n\gamma, \quad \alpha' = mn\alpha \quad (15)$$

Calculating the power using the new parameters, the power equation can be rewritten as

$$\begin{aligned} P' &= \frac{R\alpha'^2}{1 + (RC'_0\omega)^2} \frac{F_m^2}{2C^2} = \frac{R(mn\alpha)^2}{1 + (mRC_0\omega)^2} \frac{F_m^2}{2C^2} \\ &= n^2 \frac{R\alpha^2}{\frac{1}{m^2} + (RC_0\omega)^2} \frac{F_m^2}{2C^2} > n^2 \frac{R\alpha^2}{1 + (RC_0\omega)^2} \frac{F_m^2}{2C^2} = n^2 P \end{aligned} \quad (16)$$

Thus, the addition of VGCF will increase both  $g_{31}$  and  $C_0$  (or  $\varepsilon_{33}^S$ ), resulting in a remarkable increase in the harvested energy. In contrast, for the case of

PVDF/MWNT films, only increase in  $g_{31}$  was identified as discussed above, which implies that  $m=1$ ,  $n>1$  in Equations (14)–(16). Therefore, although the increase of PVDF/MWNT (0.05) films in the open circuit voltage is higher than that of PVDF/VGCF (0.05)

films, the increase of PVDF/MWNT (0.05) films in energy harvesting capability is lower compared to that of PVDF/VGCF (0.05) films.

### 3. Crystallinity

#### 3.1. XRD results

The above results confirm that the addition of nanofillers improve the piezoelectricity of PVDF matrix. The improved piezoelectric properties can be explained by desirable PVDF phase conversion during the fabrication process. The crystallinity of films before and after stretching was investigated by X-ray diffraction (XRD) method to confirm the effects of nanofillers to PVDF phase composition. The apparatus is MPX-3A (X-ray Diffractometer, Mac Science Ltd.) and the scans were carried by  $\text{CuK}\alpha$  at 40 kV and 30 mA over a range of  $2\theta$  from  $10\sim 30^\circ$ . The step was  $0.02^\circ$  and the scan speed was  $1^\circ/\text{min}$ .

Figure 9 shows the XRD spectrum of PVDF composites with various nanofiller contents. Figures 9(A) and (C) show the films before stretching and peaks exist at  $2\theta = 18.5^\circ$ ,  $19.9^\circ$ , and  $26.5^\circ$ , which correspond to (020), (110), and (021) of  $\alpha$  crystal. However, prior to stretching, there are no  $\beta$  crystal-related peaks, indicating that  $\alpha$  crystallinity is the common

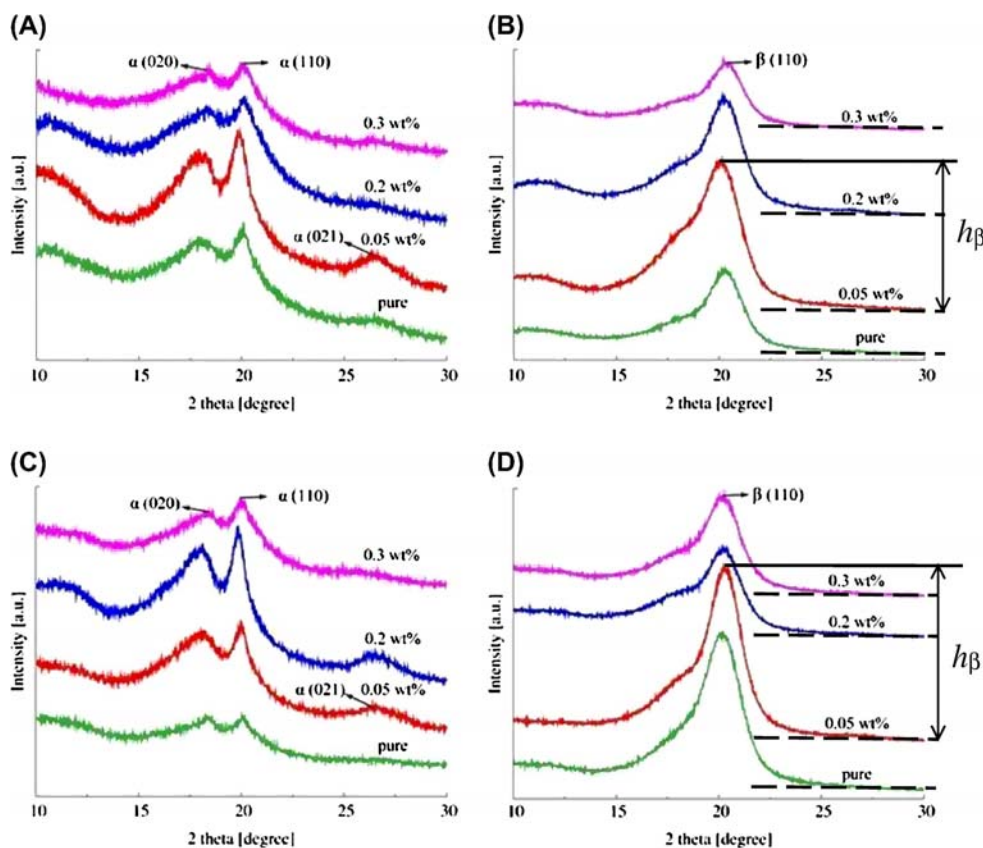


Figure 9. X-ray diffraction spectra of composite films: (A) PVDF/MWNT composite films before stretching; (B) PVDF/MWNT composite films after stretching; (C) PVDF/VGCF composite films before stretching; (D) PVDF/VGCF composite films after stretching.

state. Moreover, the addition of nanofillers can not directly induce  $\beta$  crystal (see Figure 9(A) and (C)). One interesting phenomenon in Figure 9(A) is that the most notable (0 2 1) peak of  $\alpha$  crystal exists in PVDF/MWNT(0.05) compared to other cases, which imply that a suitable nanofiller content may slightly enhance  $\alpha$  crystallinity.

For films after stretching, a peak near  $2\theta = 20.6^\circ$ , which corresponds to (1 1 0) of  $\beta$  crystal, appears, as illustrated in Figure 9(B) and (D). Moreover, in the XRD spectrum of stretched films, the peaks related to  $\alpha$  crystal disappear. It is believed that most of the  $\alpha$  crystal was converted to  $\beta$  crystal.

Sencadas et al. [6] stretched films at  $80^\circ\text{C}$  at a ratio of 5 of stretched length to original length, with a resulting  $\beta$  crystal content over 80%. Mhalgi et al. [28] casted films at  $107^\circ\text{C}$  and stretched them at a ratio of 4.2 with a resulting  $\beta$  crystal content of 95%. Therefore, in this study, the stretch ratio of length was set to be about 5. The XRD results indicate that little  $\alpha$  crystal is left. However, from Figure 9, though it is believed that the stretching leads to PVDF phase transformation, how the nanofillers affect the transformation is unclear. We can only see that, after drawing, the highest relative height  $h\beta$  measured from the peak to the baseline (dash line in Figure 9(B) and (D)) appears in the PVDF/MWNT (0.05) and PVDF/VGCF (0.05) films, which qualitatively implies the highest ratio of  $\beta$  phase content in the two cases. This evidence is consistent with the experimental results of open circuit voltage and harvested power density described previously.

### 3.2. Relationship between crystallinity and piezoelectric properties

Scheinbeim et al. [29] reported that the piezoelectric constant  $d_{31}$  is proportional to  $\beta$  crystal content. This is consistent with our work. In the present work, the addition of nanofillers improved the formation of  $\beta$  phase crystals and the bulk piezoelectric property.

In fact, much research [17,20–23] suggests that MWNT as nanofillers in PVDF matrix will work as nucleation agents for  $\beta$  phase formation. In addition, Yu et al. [30] used density functional theory to simulate the absorption energy of  $\beta$  form chains near a single-wall carbon nanotube (SWNT) surface. The results confirmed the nucleation agent effect of SWNT. In pure PVDF, the tensile load is applied on the macromolecular chain and the phase conversion is dependent on the tension and stretching speed. However, Sun et al. [31] reported that in PVDF/CNF composites, a stress concentration exists near the CNF; thus, the tensile load is mainly applied on the macromolecular chain near the PVDF/CNF interface, which is beneficial for the phase transformation. This mechanism is similar in VGCF. Naturally, much lower content of nanofillers can not form large areas of nanofiller/matrix interface, limiting the  $\beta$  crystal transformation ability. In contrast, similar to the present results, Kim et al. [20] reported that excessive MWNT addition leads to lower piezoelectric properties. He explained this phenomenon from the aspect of poling process, which includes the arrangement of dipoles and the accumulation of charge. During poling, charge accumulation occurs at the interfacial boundaries between the MWNT and polar  $\beta$  phase and nonpolar  $\alpha$  phase (or amorphous phase) due to the different current densities in the above constituents. This charge accumulation is proportional to the conductivity of PVDF, which increases with the content of MWNT. If the depolarization field resulted by charge accumulation exceeds coercive field, the  $\beta$  phase content decreases due to depoling.

Conclusively, in the present work, the content of VGCF and MWNT at 0.05 wt.% will increase  $\beta$  phase most significantly, resulting in the increases of open circuit voltage and harvested power density. On the other hand, films with nanofiller content at 0.2 and 0.3 wt.% will form less  $\beta$  phase. Possible reasons may be:

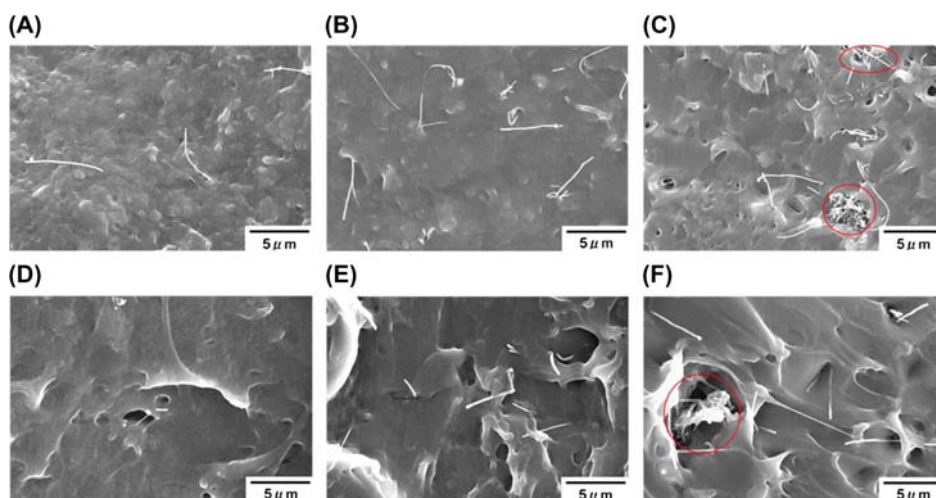


Figure 10. The SEM images of fracture surface of PVDF composite films: (A) PVDF/MWNT (0.05); (B) PVDF/MWNT (0.2); (C) PVDF/MWNT (0.3); (D) PVDF/VGCF (0.05); (E) PVDF/VGCF (0.2); (F) PVDF/VGCF (0.3).

- (1) During stretching, excessively added nanofillers may hinder the elongation of the macromolecular chain.
- (2) The charge accumulation at nanofiller/ $\beta$  crystal/ $\alpha$  crystal (amorphous area) interfaces results in a depolarization field, which becomes stronger gradually as the addition of conductive nanofillers increases.
- (4) When the nanofiller content is higher, the distribution of nanofillers is nonhomogeneous due to aggregation and the nanofillers become inefficient as nucleation agents.

#### 4. Observation of sample fracture surface

The fracture surface of PVDF composites was observed by a scanning electron microscope (SEM). Figure 10 shows the fracture surfaces of PVDF/MWNT and PVDF/VGCF films. From the SEM images, it can be seen that at contents of 0.05 and 0.2 wt.%, the MWNT and VGCF can be uniformly distributed. However, when the contents increase to 0.3 wt.%, significant aggregation is observed. This nonuniform distribution limited the nucleation effect of MWNT and VGCF, thus hindering the  $\alpha$ - $\beta$  phase transformation, resulting in 0.3 wt.% content films performing worse than pure PVDF films.

#### 5. Conclusions

To develop soft and efficient piezoelectric, environment-friendly materials, this study used PVDF as matrix, with MWNT and VGCF as nanofillers to fabricate piezoelectric composite films. Films of various compositions were fabricated and the open circuit voltage and the energy harvesting capability under dynamic strain were measured. The results indicate the enhancement of piezoelectric effects of PVDF with certain nanofiller content levels, leading to the increases of the open circuit voltage and the energy harvesting capability. Especially, the harvested power density of the PVDF/nanofiller composite films increases significantly, which shows their potential application in self-powered devices. The XRD confirmed that the

nanofillers do not significantly affect the initial melt crystallization of composites regarding to  $\beta$  crystallinity, but does play the role of  $\beta$ -phase nucleation agent during the stretching process. The SEM images show that excessive addition of nanofillers results in nonuniform distribution, limiting the nanofillers' nucleation effect. Moreover, excessive addition of nanofillers may also induce a strong depolarization field to decrease the piezoelectric effects.

### Acknowledgment

The authors are grateful to be partly supported by the Grand-in-Aid for Scientific Research (No. 22360044) from the Ministry of Education, Culture, Sports, Science, and Technology (MEXT) of Japan.

### References

- [1] Granstrom J, Feenstra J, Sodano HA, Farinholt K. Energy harvesting from a backpack instrumented with piezoelectric shoulder straps. *Smart Mater. Struct.* 2007;16:1810–1820.
- [2] Furukawa T. Ferroelectric properties of vinylidene fluoride copolymers. *Phase Trans.* 1989;18:143–211.
- [3] Hasegawa R, Takahashi Y, Chatani Y, Tadokoro H. Crystal structures of three crystalline forms of poly (vinylidene fluoride). *Polym. J.* 1972;3:600–610.
- [4] Takahashi Y, Matsubara Y, Tadokoro H. Crystal structure of form II of poly(vinylidene fluoride). *Macromolecules.* 1983;16:1588–1592.
- [5] Salimi A, Yousefi AA. Conformation changes and phase transformation mechanisms in PVDF solution-cast films. *J. Polym. Sci., Part B: Polym. Phys.* 2004;42:3487–3495.
- [6] Sencadas V, Gregorio R, JR, Lanceros-Méndez S.  $\alpha$  to  $\beta$  phase transformation and microstructural changes of PVDF films induced by uniaxial stretch. *J. Macromol. Sci. Part B Phys.* 2009;48:514–525.
- [7] Winsor DL, Scheinbeim JI, Newman BA. Effects of plasticizer on the mechanical and ferroelectric properties of uniaxially oriented  $\beta$ -phase PVF<sub>2</sub>. *J. Polym. Sci., Part B: Polym. Phys.* 1996;34:2967–2977.
- [8] Davies GR, Singh H. Evidence for a new crystal phase in conventionally poled samples of poly (vinylidene fluoride) in crystal form II. *Polymer.* 1979;20:772–774.
- [9] Ye Y, Jiang Y, Wu Z, Zeng H. Phase transitions of poly (vinylidene fluoride) under electric fields. *Integr. Ferroelectr.* 2006;80:245–251.
- [10] Scheinbeim J, Nakafuku C, Newman BA, Pae KD. High-pressure crystallization of poly (vinylidene fluoride). *J. Appl. Phys.* 1979;50:4399–4405.
- [11] Hattori T, Kanaoka M, Ohigashi H. Improved piezoelectricity in thick lamellar  $\beta$  form crystals of poly (vinylidene fluoride) crystallized under high pressure. *J. Appl. Phys.* 1996;79:2016–2022.
- [12] R Gregorio T, Jr, Chaves Pereira de Souza Nociti N, Ohigashi H. Effect of PMMA addition on the solution crystallization of the alpha and beta phases of poly (vinylidene fluoride) (PVDF). *J. Phys. D: Appl. Phys.* 1995;28:432–436.
- [13] Bhatt AS, Bhat DK, Santosh MS. Crystallinity, conductivity, and magnetic properties of PVDF-Fe<sub>3</sub>O<sub>4</sub> composite films. *J. Appl. Polym. Sci.* 2011;119:968–972.
- [14] Sun L, Li B, Zhao Y, Zhong W. Suppression of AC conductivity by crystalline transformation in poly (vinylidene fluoride)/carbon nanofiber composites. *Polymer.* 2010;51:3230–3237.
- [15] Carabineiro SAC, Pereira MFR, Pereira JN, Caparros C, Sencadas V, Lanceros-Mendez S. Effect of the carbon nanotube surface characteristics on the conductivity and dielectric constant of carbon nanotube/poly (vinylidene fluoride) composites. *Nanoscale Res. Lett.* 2011;6:302.
- [16] Vidhate S, Shaito A, Chung J, D'Souza NA. Crystallization, mechanical, and rheological behavior of polyvinylidene fluoride/carbon nanofiber composites. *J. Appl. Polym. Sci.* 2009;112:254–260.
- [17] He L, Xu Q, Hua C, Song R. Effect of multi-walled carbon nanotubes on crystallization, thermal, and mechanical properties of poly (vinylidene fluoride). *Polym. Compos.* 2010;31:921–927.
- [18] Yousefi AA. Hybrid polyvinylidene fluoride/nanoclay/MWCNT nanocomposites: PVDF crystalline transformation. *Iran. Polym. J.* 2011;20:725–733.
- [19] Dodds JS, Meyers FN, Loh KJ. Piezoelectric characterization of PVDF-TrFE thin films enhanced with ZnO nanoparticles. *IEEE Sensors J.* 2012;12:1889–1890.

- [20] Kim GH, Hong SM, Seo Y. Piezoelectric properties of poly (vinylidene fluoride) and carbon nanotube blends:  $\beta$ -phase development. *Phys. Chem. Chem. Phys.* 2009;11:10506–10512.
- [21] Lee JS, Kim GH, Kim WN, Oh KW, Kim HT, Hwang SS, Hong SM. Crystal structure and ferroelectric properties of poly (vinylidene fluoride)-carbon nanotube nanocomposite film. *Mol. Cryst. Liq. Cryst.* 2008;491:247–254.
- [22] Dang Z. High dielectric constant percolative nanocomposites based on ferroelectric poly (vinylidene fluoride) and acid-treatment multiwall carbon nanotubes. In: *IEEE 8<sup>th</sup> International Conference on Properties and Applications of Dielectric Materials*; 2006 Jun 26–30; Bali, Indonesia.
- [23] Kim GH, Hong SM. Structures and physical properties of carbon nanotube reinforced PVDF composites. *Mol. Cryst. Liq. Cryst.* 2007;472:551–559.
- [24] Dadi S, Paul R. The step-wise poling of VDF/TrFE copolymers. *Ferroelectrics*. 1996;186:255–258.
- [25] Hu N, Itoi T, Akagi T, Kojima T, Xue J, Yan C, Atobe S, Fukunaga H, Yuan W, Ning H, Surina, Liu Y, Alamusi. Ultrasensitive strain sensors made from metal-coated carbon nanofiller/epoxy composites. *Carbon*. 2013;51:202–212.
- [26] Alamusi, Xue J, Wu L, Hu N, Qiu J, Chang C, Atobe S, Fukunaga H, Watanabe T, Liu Y, Ning H, Li J, Li Y, Zhao Y. Evaluation of piezoelectric property of reduced graphene oxide (rGO)-poly (vinylidene fluoride) nanocomposites. *Nanoscale*. 2012;4:7250–7255.
- [27] Guyomar D, Badel A, Lefeuvre E, Richard C. Toward energy harvesting using active materials and conversion improvement by nonlinear processing. *IEEE Trans. Ultrason. Ferroelectr. Freq. Control*. 2005;52:584–595.
- [28] Mhalgi MV, Khakhar DV, Misra A. Stretching induced phase transformations in melt extruded poly (vinylidene fluoride) cast films: effect of cast roll temperature and speed. *Polym. Eng. Sci.* 2007;47:1992–2004.
- [29] Scheinbeim JI, Chung KT, Pae KD, Newman BA. The dependence of the piezoelectric response of poly (vinylidene fluoride) on phase-I volume fraction. *J. Appl. Phys.* 1979;50:6101–6105.
- [30] Yu S, Zheng W, Yu W, Zhang Y, Jiang Q, Zhao Z. Formation mechanism of  $\beta$ -phase in PVDF/CNT composite prepared by the sonication method. *Macromolecules*. 2009;42:8870–8874.
- [31] Sun LL, Li B, Zhang ZG, Zhong WH. Achieving very high fraction of  $\beta$ -crystal PVDF and PVDF/CNF composites and their effect on AC conductivity and microstructure through a stretching process. *Eur. Polymer J.* 2010;46:2112–2119.